A STUDY OF THE LOAD-SHORTENING RELATIONSHIP OF AXIALLY LOADED PIN ENDED STRUTS

VIJAY REWAL

A DISSERTATION

in the

Faculty of Engineering

Presented in partial fulfilment of the requirements for
the Degree of Master of Engineering at
Concordia University, Sir George Williams Campus
Montreal, Canada

September 1976

ABSTRACT

ABSTRACT

VIJAY REWAL

A STUDY OF THE LOAD-SHORTENING RELATIONSHIP
OF AXIALLY LOADED PIN ENDED STRUTS

A simple analysis predicting the load-shortening relationship of axially loaded simply supported struts is presented.

Tests were conducted to study the actual behaviour of struts with varying slenderness ratios and different cross-sectional shapes. The theoretical behaviour of the struts is found to be in reasonable agreement with the test results for practical design purposes.

The problems encountered while performing the tests are also examined.

Earlier works are found to be in agreement with the Elastic theory.

ACKNOWLEDGEMENTS

ACKNOWLEDGEMENTS

The work presented in this dissertation was carried out under the direct supervision of Professor C. Marsh, to whom the author wishes to express his deepest gratitude for his guidance and encouragement.

The facilities provided by the Structures Laboratory of Concordia University, Sir George Williams Campus, are gratefully acknowledged.

Thanks are also due to Miss Louise Lapierre for typing this manuscript.

CONTENTS

TABLE OF CONTENTS

FIGURES

LIST OF FIGURES

TABLES

LIST OF TABLES

NOTATIONS

NOTATIONS

The following symbols, which are arranged alphabetically, have been adopted for use in the analytical work and are defined where they appear first.

c	distance from Centre of Gravity to extreme fibre
ds	element length of bowed strut
dx	element length of straight strut
r	radius of gyration
t	thickness of tube
A	cross sectional area
I	moment of inertia
L	length
P	axial load
Pe	Euler load
S	section modulus
Z	plastic section modulus
O.D.	outside diameter
δ	axial shortening of a strut
δb	difference between the length of the straight strut and the bowed strut
Δ	lateral deflection
λ	slenderness ratio
ε	effective axial strain
σ_e	mean axial stress
σ_y	Euler stress
σ	yield stress

CHAPTER 1

INTRODUCTION

CHAPTER 1

INTRODUCTION

Space trusses are used to provide large unobstructed covered areas for storage buildings, exhibition halls, airplane hangars, and similar structures. The economics of the utilization of space trusses can be improved by making full use of the strength of the truss in the post buckling domain.

The behaviour of the space truss in the inelastic range is not fully understood despite the importance of this structural element. Very few researchers (1, 2, 3) have conducted experiments to study the load-collapse behaviour of the space truss. The reserve of strength between working load and collapse load has not been fully established and, therefore, it cannot be safely used by the designers.

The ultimate capacity of the space truss depends upon the behaviour and strength of the members after buckling. Yielding of tensile members leads to redistribution of forces, but compression member instability may lead to a "brittle" type failure (3). The buckling of compression members is most likely to govern the ultimate design of the space-truss. The post-yield behaviour of such members depends upon their slenderness ratio.

The post-yield behaviour of slender struts in isolation and the change of length involved as the strut bows, are experimentally examined herein. A simple formula is suggested to predict the load/shortening relationship of struts.

CHAPTER 2

EARLIER WORKS

CHAPTER 2

EARLIER WORKS

Only very recently have the designers realized the importance of the change of length of struts in the post buckling state. The most important work on this is being conducted in Australia and Germany.

Schmidt (1, 3) has probably stressed more than anyone else the importance in ultimate design of space-trusses of the post buckling behaviour of struts. He conducted some experiments (1) in isolation on compression members. For his tests he used the Triodetic System in which the members have flattened ends. The effective length used was the length between the flattened faces. This gave the slenderness ratio as 67. He gave an axial load, P, versus axial deformation, δ, curve Fig. 2.1.

In this paper (1) Schmidt did not give very many details of the experiments. Along with the experimental curve in Fig. 2.1 he also gave a theoretical curve. But he did not mention how he arrived at this theoretical curve. For each member tested, he also measured the E value, which was used in predicting the load/shortening relationship.

Schmidt's paper (1) did not give any results for the experimental curve Fig. 2.1. From the given experimental curve Fig. 2.1 these values i.e., the axial deformation at a particular value of axial load, were extracted in Table 2.1. Knowing the member properties, the values of axial deformations were calculated in the elastic range using the Hooke's Law $\delta = \frac{PL}{AE}$, at any particular value of axial load P. The experimental values of δ below the Euler load were then compared with the theoretical values of δ. Table 2.2.

The experimental values, as obtained from Fig. 2.1 and the calculated values of δ, were found to be different Table, 2.2. We, in our experiments, encountered similar problems - the experimental values of δ in the elastic state were different from the proven theoretical values of δ.

Wolf (2) uses the initial-stress method of iteration to use the load-shortening relationship, Fig. 2.2, for rectangular struts. He does not mention how he arrived at the various values used in the above method, neither does he make any mention of having performed experiments in isolation on the struts.

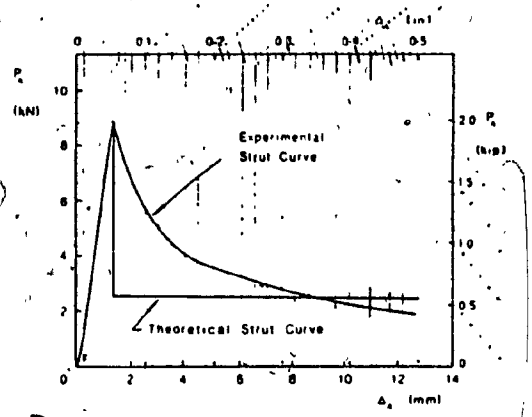

Fig. 2.1 Load shortening of struts (1)

TABLE 2.1 (1)

SCHMIDT (1) TEST RESULT VALUES

Test results as extracted from Fig. 2.1.

AXIAL LOAD P kps	AXIAL DEFORMATION δ in.	MEMBER PROPERTIES
0.3	0.01	Circular hollow tube
0.7	0.02	O.D. = .5"
1.1	0.03	t = .06"
1.55	0.04	L = 11.89"
2.0	0.05	A = 0.086 sq.in.
		E = 7221 ksi

TABLE 2.2 (1)

COMPARISON WITH SCHMIDT (1) TEST

Euler load $P_e = \frac{\pi^2 EI}{L^2}$

$= 2.92$ kps

Euler stress $\sigma_e = \frac{2.92}{.086}$

$= 33.95$ ksi

AXIAL LOAD	AXIAL DEFORMATION Experimental	AXIAL DEFORMATION Theoretical
P Kps	δ in.	$\delta = \frac{PL}{AE}$ in.
0.3	.01	0.0057
0.7	.02	0.0134
1.1	.03	0.021
1.55	.04	0.029
2.0	.05	0.038

CHAPTER 3

LOAD SHORTENING RELATIONSHIP OF STRUTS

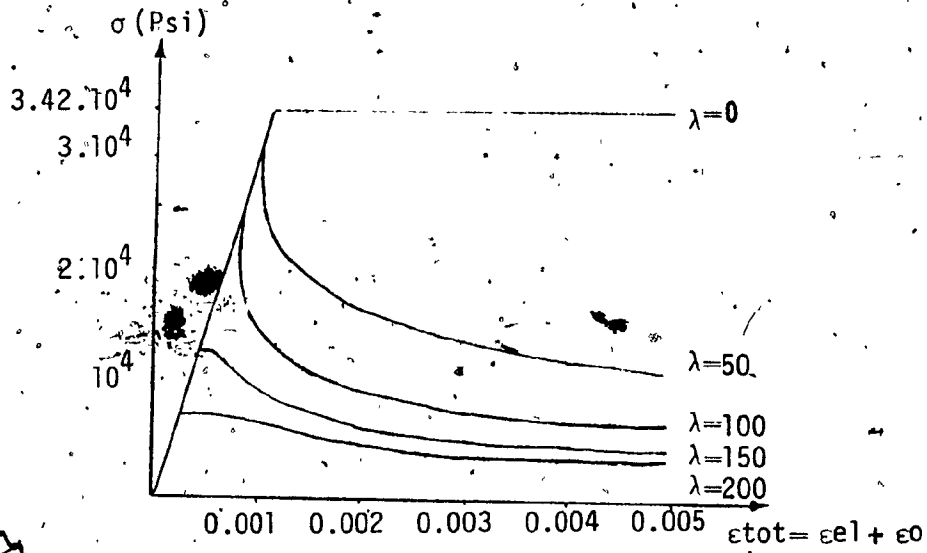

Fig. 2.2 Load-axial deflection relationship of bar in compression (2)

CHAPTER 3

LOAD SHORTENING RELATIONSHIP OF STRUTS

3.1 GENERAL

Struts can basically be divided into two main categories:

a) Intermediate (elasto-plastic);

b) Slender struts (elastic).

Euler in 1757 published his famous formula on the form of an elastic strip under end loading (4)

$$P_e = \frac{\pi^2 EI}{L^2} \quad \ldots\ldots\ldots\ldots\ldots\ldots 3.1$$

for the critical axial compressive load Pe which could be sustained by an initially straight uniform elastic bar of length L and Young's modulus E, where I is the relevant second moment of area of the cross section about a centroidal axis. For compressive load below Pe, the sideways bow of the column is zero. This Euler load is used for the design of compression members in elastic range. Another form of the Euler's formula is

$$\sigma_e = \frac{\pi^2 E}{(L/r)^2} \quad \ldots\ldots\ldots\ldots\ldots\ldots 3.2$$

Here σ_e is the critical load divided by the cross-sectional area A of the column, and r is the radius of gyration of the cross-section defined by $I = Ar^2$. The quantity L/r is called the Slenderness Ratio.

When the mean axial stress exceeds the elastic limit, the Euler expression may be extended into the elasto-plastic range by replacing E by the tangent modulus E_t

$$\sigma_{cr} = \frac{\pi^2 E_t}{(L/r)^2} \qquad \ldots\ldots\ldots\ldots 3.3$$

In our case we are mainly concerned with slender struts as the compression members generally used in the space truss belong to this category.

3.2 BUCKLING OF SLENDER STRUTS

The behaviour of slender struts is very different from that of stocky struts. Slender struts buckle initially at an axial load without any face reaching the yield stress.

Consider an axially loaded strut as shown in Fig. 3.1. As the load P is steadily increased, the strut remains straight until it reaches Pe. The strut begins to bow after reaching the Euler load Pe and the stress deviates from uniform stress. Assuming this ideal relationship, shown in Fig. 3.2, between axial load and the buckled configuration of the strut, the axial load can be said to be limited either by buckling

$$P = \frac{\pi^2 EI}{L^2}$$

$$\frac{P}{A} = \sigma_e \qquad \ldots\ldots\ldots\ldots 3.4$$

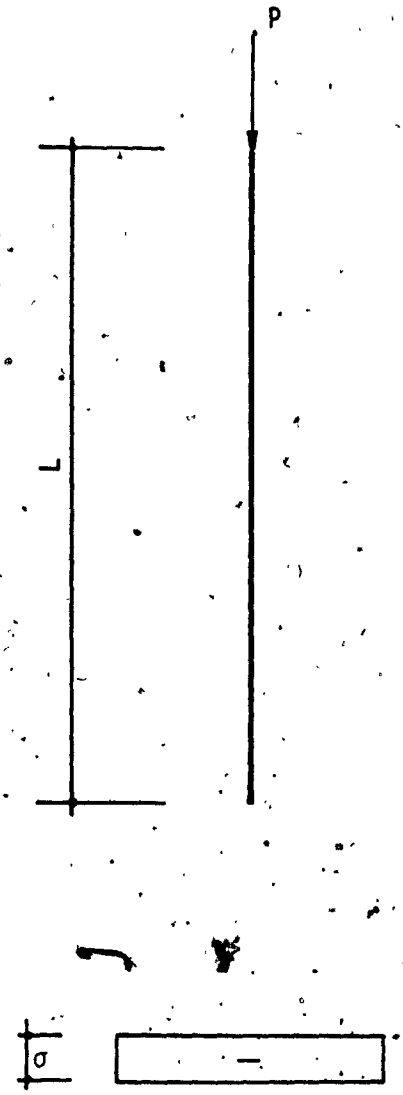

Fig. 3.1 Uniform Stress Diagram

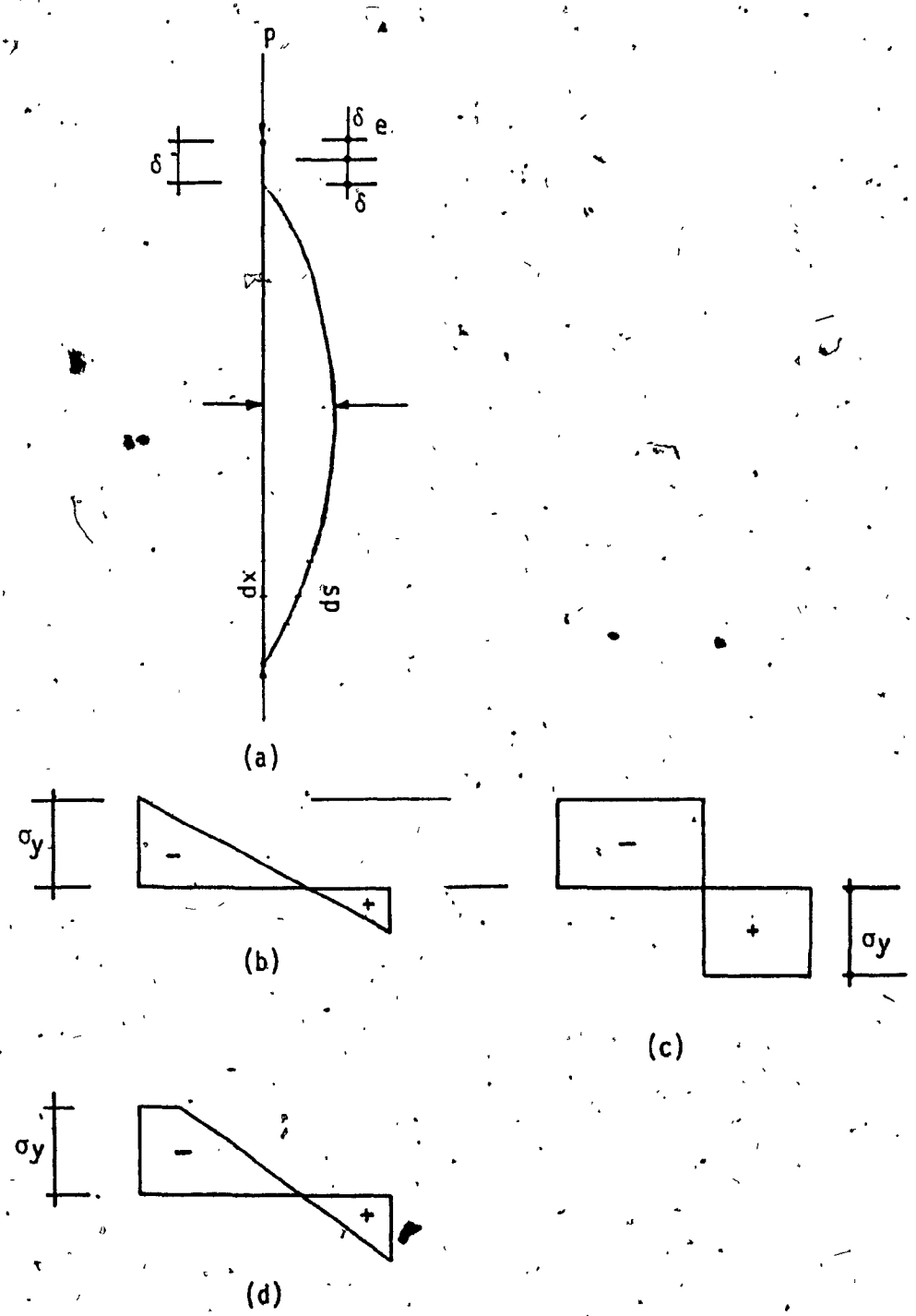

Fig. 3.2 Stress Diagram

or by stress reaching the yield stress at the centre

$$\frac{P}{A}+\frac{P\,\Delta\,c}{I} = \sigma_y \qquad \ldots\ldots\ldots\ldots\ldots\ldots 3.5$$

where c = distance from C.G. to extreme fibre

Δ = lateral deformation at the centre of the strut.

The relationship between the bow of the strut and the mean axial stress is also shown in Fig. 3.3.

Equation 3.5 can also be written as:

$$\sigma + \frac{P\,\Delta\,c}{Ar^2} = \sigma_y \qquad \ldots\ldots\ldots\ldots\ldots\ldots 3.5A$$

$$\frac{P\,\Delta\,c}{Ar^2} = \sigma_y - \sigma$$

$$\frac{\Delta\,c}{r^2} = \frac{\sigma_y}{\sigma} - 1 \qquad \left[\frac{P}{A} = \sigma\right]$$

$$\frac{\Delta}{r} = \left(\frac{\sigma_y}{\sigma} - 1\right)\frac{r}{c} \qquad \ldots\ldots\ldots\ldots\ldots 3.6$$

The effective axial strain can be given as

= strain due to axial load + strain due to the two ends of the strut coming together due to the lateral deflection.

$$\frac{\sigma}{E} + \frac{\delta b}{L} \qquad \left[\delta b = \text{difference between the length of the straight strut and the bowed strut}\right]$$

Consider an element ds of the bowed strut and dx of the straight strut. Fig. 3.2 a.

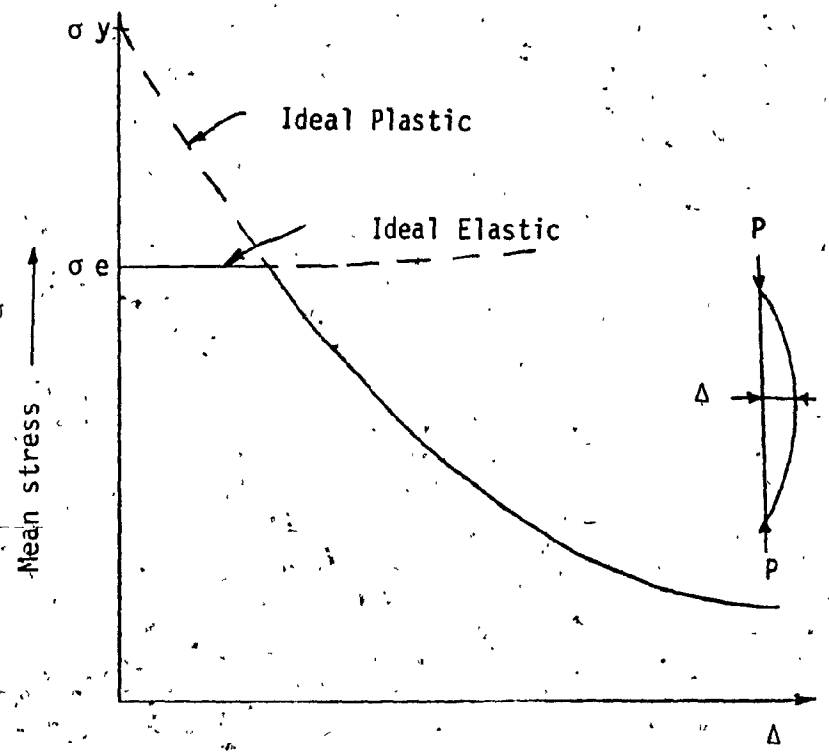

Fig. 3.3 Axial stress - bow Relationship

$$ds = dx\sqrt{1+\left(\frac{dy}{dx}\right)^2}$$

$$= dx\left[1+\left(\frac{dy}{dx}\right)^2\right]^{\frac{1}{2}}$$

Expanding and neglecting the higher powers

$$= dx\left[1+\frac{1}{2}\left(\frac{dy}{dx}\right)^2+ \text{----}\right]$$

$$ds = dx+\frac{1}{2}\left(\frac{dy}{dx}\right)^2 dx$$

$$ds - dx = \frac{1}{2}\left(\frac{dy}{dx}\right)^2 dx$$

$$\therefore \delta b = \frac{1}{2}\int_0^L \left(\frac{dy}{dx}\right)^2 dx, \text{ integrating over}$$

length L of the strut. The deflected form of the strut can be represented by the first term of the Fourier Series.

$$y = \Delta \frac{\text{Cos. } \pi x}{L}$$

$$\therefore \frac{d^2y}{dx^2} = -\frac{\Delta\pi^2}{L^2}\,\frac{\text{Cos. } \pi x}{L}$$

Substituting in the expression for δb and integrating

$$\delta b = \frac{\pi^2}{4L} x \Delta^2$$

$$\text{or } \frac{\delta b}{L} = \frac{\pi^2}{4} x \left(\frac{\Delta}{L}\right)^2$$

$$\text{or } \varepsilon = \frac{\delta}{L} = \frac{\sigma}{E} + \frac{\pi^2}{4}\left(\frac{\Delta}{L}\right)^2$$

$$\varepsilon = \frac{\sigma}{E} + \left(\frac{\pi}{4}\right)^2 \left(\frac{\Delta^2}{\pi^2 EI/\sigma_e A}\right) \qquad \left[L^2 = \frac{\pi^2 EI}{\sigma_e A}\right]$$

$$= \frac{\sigma}{E} + \left(\frac{\pi}{4}\right)^2 \left(\frac{\Delta^2}{\pi^2 E\ Ar^2/\sigma_e A}\right) \qquad \left[I = Ar^2\right]$$

$$= \frac{\sigma}{E} + \frac{\sigma_e}{4} \times \frac{\Delta^2}{r^2} \times \frac{1}{E}$$

$$\varepsilon E = \sigma + \frac{\sigma_e}{4} \times \left(\frac{\Delta}{r}\right)^2 \qquad \ldots\ldots\ldots\ldots\ 3.7$$

Putting the value of $\frac{\Delta}{r}$ from 3.6, the expression 3.7 can be written as:

$$\varepsilon E = \sigma + \frac{\sigma_e}{4}\left[\frac{\sigma_y^2}{\sigma^2} + 1 - \frac{2\sigma_y}{\sigma}\right]\frac{r^2}{c^2}$$

$$\frac{\varepsilon E}{\sigma_y} = \frac{\sigma}{\sigma_y} + \frac{\sigma_e}{4\sigma_y}\left[\frac{\sigma_y}{\sigma} - 1\right]^2 \frac{r^2}{c^2} \quad \ldots\ 3.8$$

or $$\frac{\delta}{L}\left(\frac{E}{\sigma_y}\right) = \frac{\sigma}{\sigma_y} + \frac{\sigma_e}{4\sigma_y}\left[\frac{\sigma_y}{\sigma} - 1\right]^2 \frac{r^2}{c^2} \quad \ldots\ 3.9$$

This expression can be further simplified by assuming that $\frac{r}{c}$ is approximately equal to 1.

$$\varepsilon\left(\frac{E}{\sigma_y}\right) = \frac{\sigma}{\sigma_y} + \frac{\sigma_e}{4\sigma_y}\left[\frac{\sigma_y}{\sigma} - 1\right]^2 \qquad \ldots\ldots\ 3.10$$

This expression is plotted for various values of $\frac{\sigma_e}{\sigma_y}$ in Fig. 3.4.

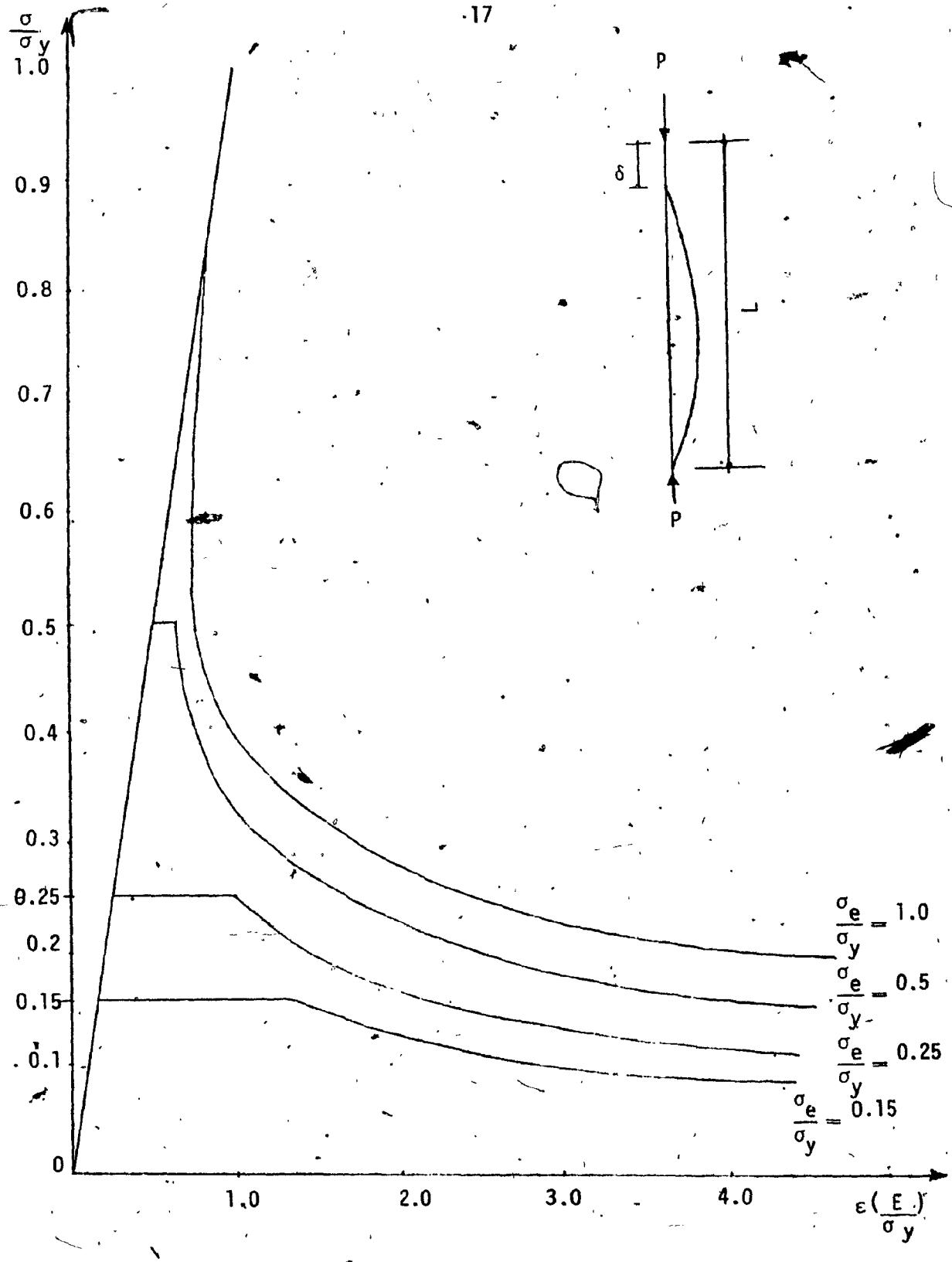

Fig. 3.4. Axial stress-strain relationship

The fully plastic state, see Fig. 3.2 d, may be expressed approximately as

$$\left(\frac{\sigma}{\sigma_y}\right)^2 + \frac{\sigma}{\sigma_y} \times \frac{A\Delta}{Z} = 1 \quad \ldots\ldots\ldots\ldots\ldots\ldots \quad 3.11$$

Z = Plastic Section Modulus

let $\frac{Z}{A} = r$ then

$$\left(\frac{\sigma}{\sigma_y}\right)^2 + \frac{\sigma}{\sigma_y} \times \frac{\Delta}{r} = 1$$

or $$\frac{\Delta}{r} \times \frac{\sigma}{\sigma_y} = 1 - \left(\frac{\sigma}{\sigma_y}\right)^2$$

$$\frac{\Delta}{r} = \frac{\sigma_y}{\sigma} - \frac{\sigma}{\sigma_y} \quad \ldots\ldots\ldots\ldots\ldots\ldots \quad 3.12$$

Substituting this value of $\frac{\Delta}{r}$ in expression 3.7

$$\varepsilon E = \sigma + \frac{\sigma e}{4}\left(\frac{\sigma_y}{\sigma} - \frac{\sigma}{\sigma_y}\right)^2$$

or $$\varepsilon\left(\frac{E}{\sigma_y}\right) = \frac{\sigma}{\sigma_y} + \frac{\sigma e}{4\sigma_y}\left(\frac{\sigma_y}{\sigma} - \frac{\sigma}{\sigma_y}\right)^2 \ldots\ldots \quad 3.13$$

and using correct values of Z, A and r

$$\varepsilon\left(\frac{E}{\sigma_y}\right) = \frac{\sigma}{\sigma_y} + \frac{\sigma e}{4\sigma_y}\left(\frac{\sigma_y}{\sigma} - \frac{\sigma}{\sigma_y}\right)^2 \times \frac{Z^2}{I^2} \times r^2$$

The above expressions are essentially qualitative in nature to indicate the behaviour of an axially loaded strut which, in practice, will vary with the shape of the cross section and the length of the strut.

It can be seen that using expression 3.10, the slope of the curve at $\sigma = \sigma_e$ is vertical when $\frac{\sigma_e}{\sigma_y} = 0.5$.

This is the limit usually assumed of the elasto-plastic range for struts and suggests that any strut shorter than this cannot be expected to provide any useful post-buckling plateau.

The effective "plastic" axial strain, ε_p, at the end of the "plateau" for a limit load Po equal to 90% of the true capacity is approximately given by

$$\varepsilon_p \left(\frac{E}{\sigma_y} \right) = \frac{\sigma_y}{4\sigma_e} - 0.5 \quad \ldots\ldots\ldots\ldots\ldots\ldots\ldots\ldots \quad 3.14$$

With these load/shortening relationships, the value of the ultimate load analysis for space trusses becomes questionable, unless the requirements for a post-buckling capability to shorten under constant load are minimized.

It follows that an ideal design in which a number of members are proportioned to fail at the same time cannot be based on the maximum strut capacity. The value adopted will have to be a

function of the probable variation between nominally equal member loads and the length of the available load/shortening plateau.

CHAPTER 4

TESTS

CHAPTER 4

TESTS

The first series of tests was started in the beginning of February, 1979. All the tests were conducted in the Structures Laboratory at the Sir George Williams Campus.

4.1 TEST OBJECTIVES

The principal object of these tests was to obtain the strut shortening or change in length of the strut as it was gradually loaded axially beyond the elastic limits and to compare the test results with the results obtained from the proposed theory. An additional objective was to compare the behaviour of the test specimen, i.e. the load shortening relationship, the Euler load, within the elastic range with the existing proven theories. For this purpose, continuous measurements of load, deflection and axial shortening were taken.

4.2 TEST PROGRAMME

The test specimens included a variety of shapes and slenderness ratios. In the first series of tests, angle (L) and circular hollow tube members were tested. In the final test series square and circular bars were tested. It was also decided to conduct tests on a particular specimen, plot the curves and check the results before proceeding on to testing the next set of specimens. The results of the tests conducted on the circular hollow tube sections

are not included in this Study as the test conditions deviated from the assumed study conditions. Moreover, the tube was not made from high strength structural alloy.

4.3 TESTING MACHINES

The tests were conducted on two separate testing machines. The angle sections (L) were all tested in the 120,000 lb. Tinius Olsen testing machine (Machine 1). This machine did not have any plotter or direct displacement reading device attached to it.

The square bar and the circular bar were tested in a 60,000 lb. Tinius Olsen machine (Machine 2). This machine has a plotter attached which automatically plotted the load vs. platten displacement. The machine is capable of plotting the load shortening relationship on different scales.

4.4 DESCRIPTION OF TESTS

4.4.1 BEARING TYPE 1

The end bearing for the angle section (L) consisted of a 6in. x 6in. x 1½in. thick steel bearing plate having a knife edge at each end, see Fig. 4.1. The distance from the top of the plate to the underside of the knife edge was added to the length of the strut.

The knife edge was formed at an angle of 45^{o} to the horizontal plate surface. Each end bearing plate had a small centrally located hole in it. A steel plate cut to the shape and size in plan to the

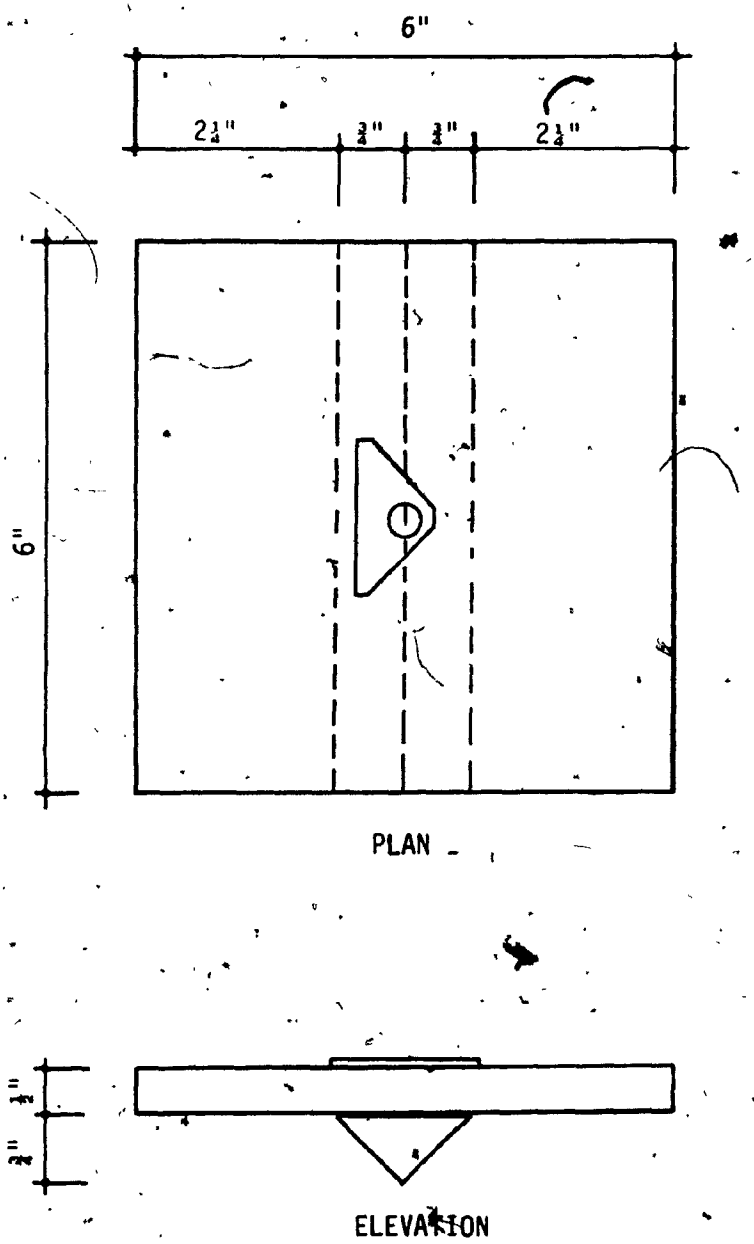

Fig. 4.1 Bearing Type 1

inside dimensions of the specimen was screwed to the plate at the centrally located hole in the plate. The test specimen was held tight against this screwed plate at both top and bottom. This ensured that the test specimen was loaded axially. This bearing is called Bearing 1.

4.4.2 BEARING TYPE 2 and TYPE 3

Bearing Type 2 consisted of a 3/16in. thick circular plate of 1½in. diameter with a circular opening in the centre of the plate such that a steel ball of 3/8in. diameter could be seated in the opening. This circular plate and ball combination was also used for the top end bearing. A circular recess was made at each end of the specimens to accommodate the ball bearing. Before testing each specimen, the ball bearings, the circular openings in the plates and the grooves at each end were well greased. Fig.

Bearing Type 3 consisted of a frustum of a cone ½in. diameter at the bottom and 1½in. diameter at the top. See Fig. 4.3. A circular (3/4in. diameter) recess ¼in. deep in the top of the cone accommodated the specimen. The bottom face of the cone was recessed to accept the ball bearing.

4.5 METHODS OF MEASUREMENT

Using Machine 1, the load indicated by the machine at any particular time in the loading history of the specimen, the length of the specimen and the lateral deflection of the specimen at that time was read and recorded simultaneously. This continuous process of

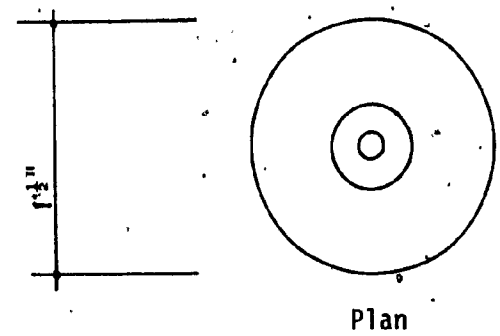

Plan

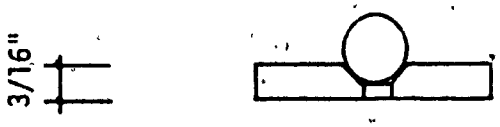

Elevation

Fig. 4.2 Bearing Type 2

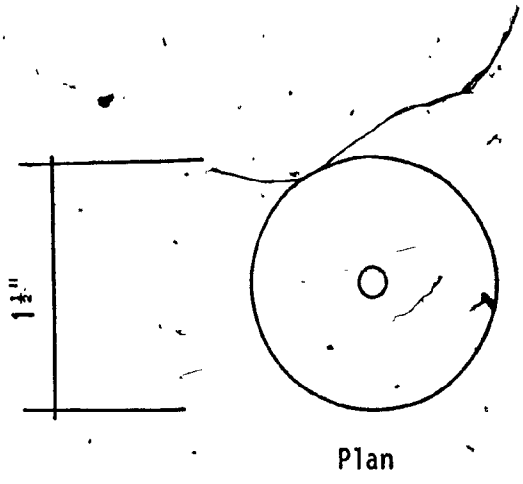

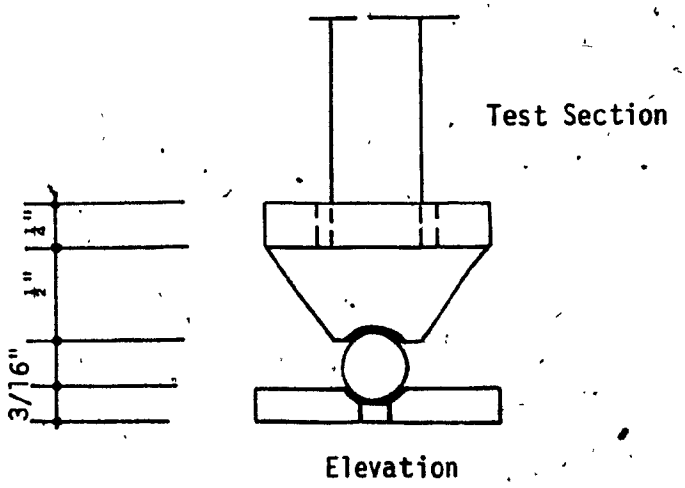

Fig. 4.3 Bearing Type 3

readings and recordings was carried on till the member collapsed or the bearing plate came in contact with the machine plate thereby stopping any further rotation. The change of length was read on a dial gauge attached to the top of the machine plate. The central deflection of the specimen was read on a dial gauge attached to the mid-length of the specimen. See Fig. 4.4. The length of the specimen was taken as the distance between the two knife edges when the load was initiated.

The load would be called out and the dial gauge readers would read and record the loading at that load. These readings were recorded as accurately as possible. It was not always possible to predict the direction of buckling of the specimen which added to the problem of locating the dial gauge in relation to the bow.

Machine 2 had a plotter which recorded the load-shortening relationship as the load was applied and no additional measurements were required.

4.6 RELATED PROBLEMS

It was not very easy to locate the top knife edge bearing plate centrally and accurately above the bottom knife edge plate as there was no mark on the top plate of the machine locating the axis of loading. The top knife edge was located as centrally as possible by approximately locating the centre of the machine plate by measurements.

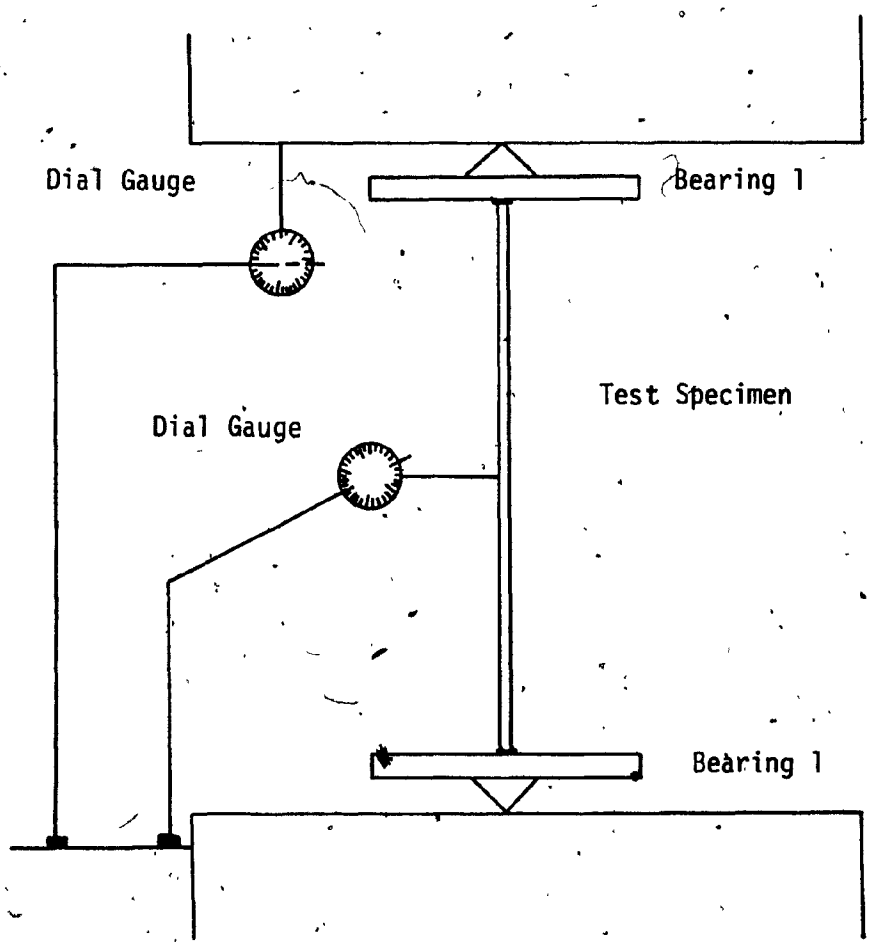

Fig. 4.4 Dial Gauge Location

The loading axis of the member could only be checked after putting an initial load on the member when the load was just initiated.

CHAPTER 5

TEST RESULTS AND COMPARISON WITH "THEORY"

CHAPTER 5

TEST RESULTS AND COMPARISON WITH THEORY

TABLE 5.1
TEST MEMBERS

MEMBER NO.	CROSS SECTION	L in.	BEARING USED	σ_y ksi
1	1 in. x 1 in. x 1/8 in. L	30	1	40
2	1 in. x 1 in. x 1/8 in. L	24	1	40
3	1 in. x 1 in. x 1/8 in. L	18	1	40
4	½ in. Dia. ○	22	2	35
5	½ in. Dia. ○	16	2	35
6	½ in. x ½ in. □	19	3	35
7	½ in. x ½ in. □	14	3	35

All specimens tested were medium strength aluminum alloy AA 6061 - T6

TABLE 5.2

MEMBER 1, BEARING 1

TEST RESULTS

P kips	Δ in.	δ in.	MEMBER PROPERTIES	$\frac{\sigma}{\sigma_y}$
			ANGLE SECTION	
0.280	0.08	0.015	1in.x1in.x1/8in.	
0.500	0.049	0.022	A = .24sq.in.	
0.750		0.049	L = 30+2.5 in.	
0.800		0.02	σ_y = 40 ksi	
0.850		0.132	E = 10^4 ksi	0.088 *
0.780		0.184	$\frac{L}{r} = \frac{32.5}{.2}$	0.08
0.750		0.195		0.078
0.680		0.235	= 162.5	0.07
			Pe= 0.89 kip	
			$\sigma_e = \frac{\pi^2 E r^2}{L^2}$	
			= 3.74 ksi	
			$\frac{\sigma_e}{\sigma_y}$ = 0.09	

TABLE 5.2 cont'd.

MEMBER 1, BEARING 1

TEST RESULTS $\varepsilon\left(\frac{E}{\sigma y}\right) = \delta \times 8.3$	ELASTIC THEORY $\varepsilon\left(\frac{E}{\sigma y}\right) = \frac{\sigma}{\sigma y} + \left(\frac{\sigma e}{4\sigma y}\right)\left(\frac{\sigma y}{\sigma} - 1\right)^2 \frac{r^2}{c^2}$ $= \frac{\sigma}{\sigma y} + .023\left(\frac{\sigma y}{\sigma} - 1\right)^2 \times .47$
* 1.09	1.24
1.52	1.46
1.61	1.58
1.95	1.93

TABLE 5.3

MEMBER 2, BEARING 1

TEST RESULTS

P kips	Δ in.	δ in.	MEMBER PROPERTIES	$\frac{\sigma}{\sigma_y}$
			ANGLE SECTION	
0.250	0	0.014	1in.x1in.x1/8in.	
0.500	0.015	0.021	A = .24sq.in.	
0.750	0.048	0.027	L = 24+2.5in.	
1.000	0.109	0.034	= 26.5 in.	
1.100	0.175	0.039	σ_y = 40 ksi	
1.150	0.226	0.042	E = 10^4 ksi	
1.200	0.674	0.05	r = 0.2 in.	
1.250	0.66	0.07	$\frac{L}{r}$ = 132.5	
1.150	0.066	0.099		0.119 *
1.100		0.111	Pe = 1.34 kps	0.114
0.975		0.137	$\sigma_e = \frac{\pi^2 Er^2}{L^2}$	0.1
0.850		0.182		0.088
			= 5.62 ksi	
			C = .29 in.	
			$\frac{\sigma_e}{\sigma_y}$ = 0.14	

TABLE 5.3 cont'd.

MEMBER 2, BEARING 1

TEST RESULTS $\varepsilon_\circ \left[\frac{E_\circ}{\sigma y}\right] = \delta \times 10.41$	ELASTIC THEORY $\varepsilon \left[\frac{E}{\sigma y}\right] = \frac{\sigma}{\sigma y} + \frac{\sigma e}{4\sigma y}\left[\frac{\sigma y}{\sigma} - 1\right]^2 \frac{r^2}{c^2}$ $= \frac{\sigma}{\sigma y} + .035\left[\frac{\sigma y}{\sigma} - 1\right]^2 \times .47$
* 1.03	1.0
1.156	1.1
1.42	1.39
1.89	1.83

$\frac{P}{\sigma}$	Δ	$\frac{\Delta}{\sigma}$
1.08	0	0
2.17	.015	.007
3.76	.048	.015
4.34	.109	.025
4.78	.175	.037
5.0	.226	.045

$$\sigma_e = \frac{.037}{.0065}$$

5.69 ksi

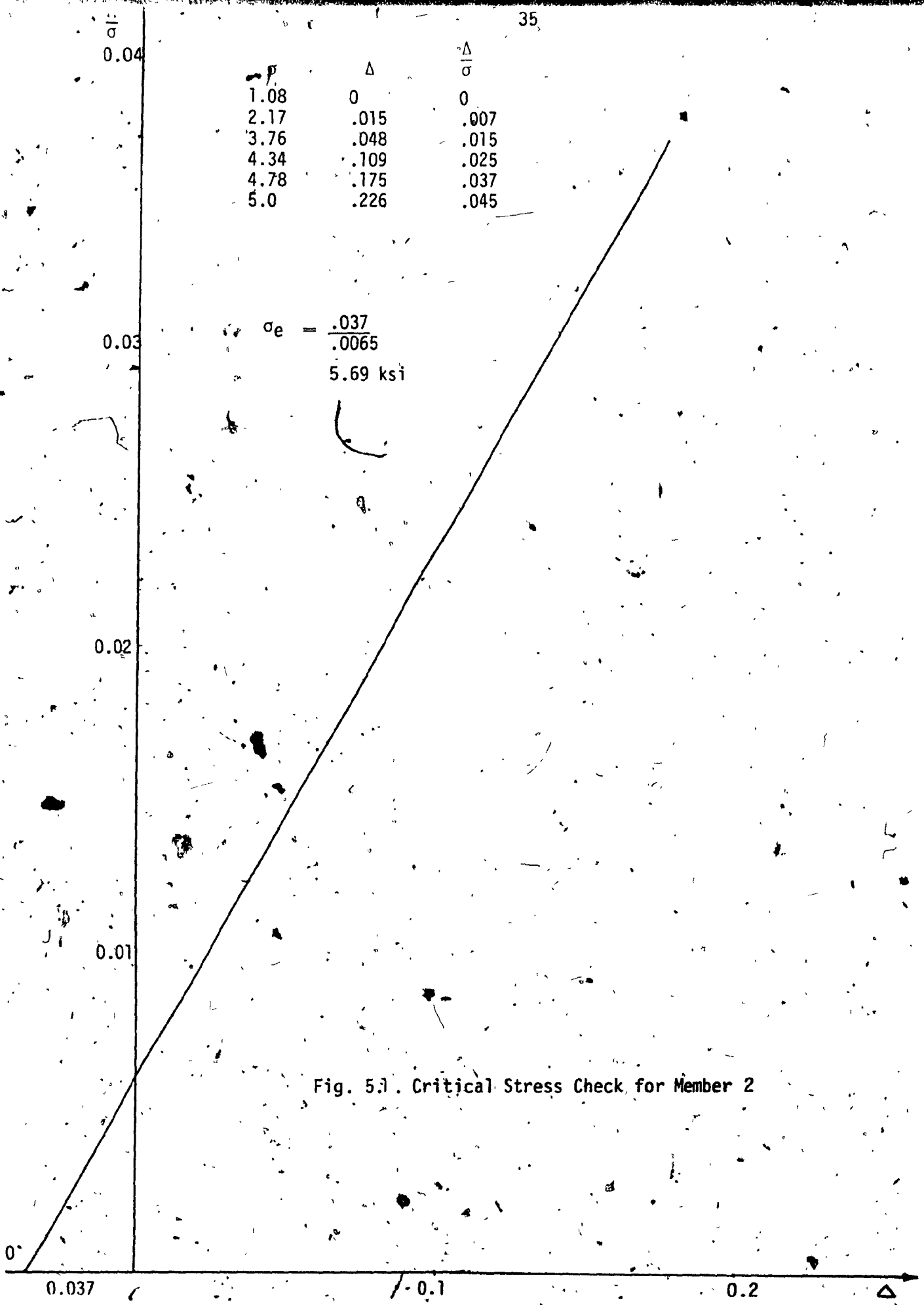

Fig. 5.1. Critical Stress Check for Member 2

TABLE 5.4

MEMBER 3, BEARING 1

TEST RESULTS

P kips	Δ in	δ in.	MEMBER PROPERTIES	$\frac{\sigma}{\sigma_y}$
			ANGLE SECTION	
0.550	0	0.019	1in.x1in.x1/8inL	
0.650	0	0.021	A = 0.24sq.in.	
0.750	0	0.023	L = 18+2.5in.	
0.850	0	0.026	σ_y = 40 ksi	
1.000	0	0.028	E = 10^4 ksi	
1.125	0	0.03	r = 0.2in.	
1.250	0.011	0.033	$\frac{L}{r}$ = 102.5	
1.400	0.011	0.035		
1.500	0.02	0.037	Pe = 2.25 kips	
1.600	0.02	0.039	$= \frac{\pi^2 Er^2}{L^2}$	
1.750	0.035	0.041		
1.950	0.072	0.046		
2.100		0.049	= 9.39 ksi	0.21 *
1.950		0.050	= .29 in.	0.2
1.880		0.052	$\frac{\sigma_e}{\sigma_y}$ =0.23	0.195
1.750		0.058		0.182
1.550		0.065		0.161
1.300		0.083		0.135
1.050		0.13		0.11

TABLE 5.4 cont'd.

MEMBER 3, BEARING 1

TEST RESULTS $\varepsilon\left[\frac{E}{\sigma_y}\right] = \delta \times 13.89$	ELASTIC THEORY $\varepsilon\left[\frac{E}{\sigma_y}\right] = \frac{\sigma}{\sigma_y} + \frac{\sigma_e}{4\sigma_y}\left[\frac{\sigma_y}{\sigma} - 1\right]^2 \frac{r^2}{c^2} = \frac{\sigma}{\sigma_y} + .058\left[\frac{\sigma_y}{\sigma} - 1\right]^2 \times .47$
* 0.63	0.56
0.69	0.623
0.72	0.65
0.80	0.73
0.90	0.89
1.15	1.11
1.80	1.80

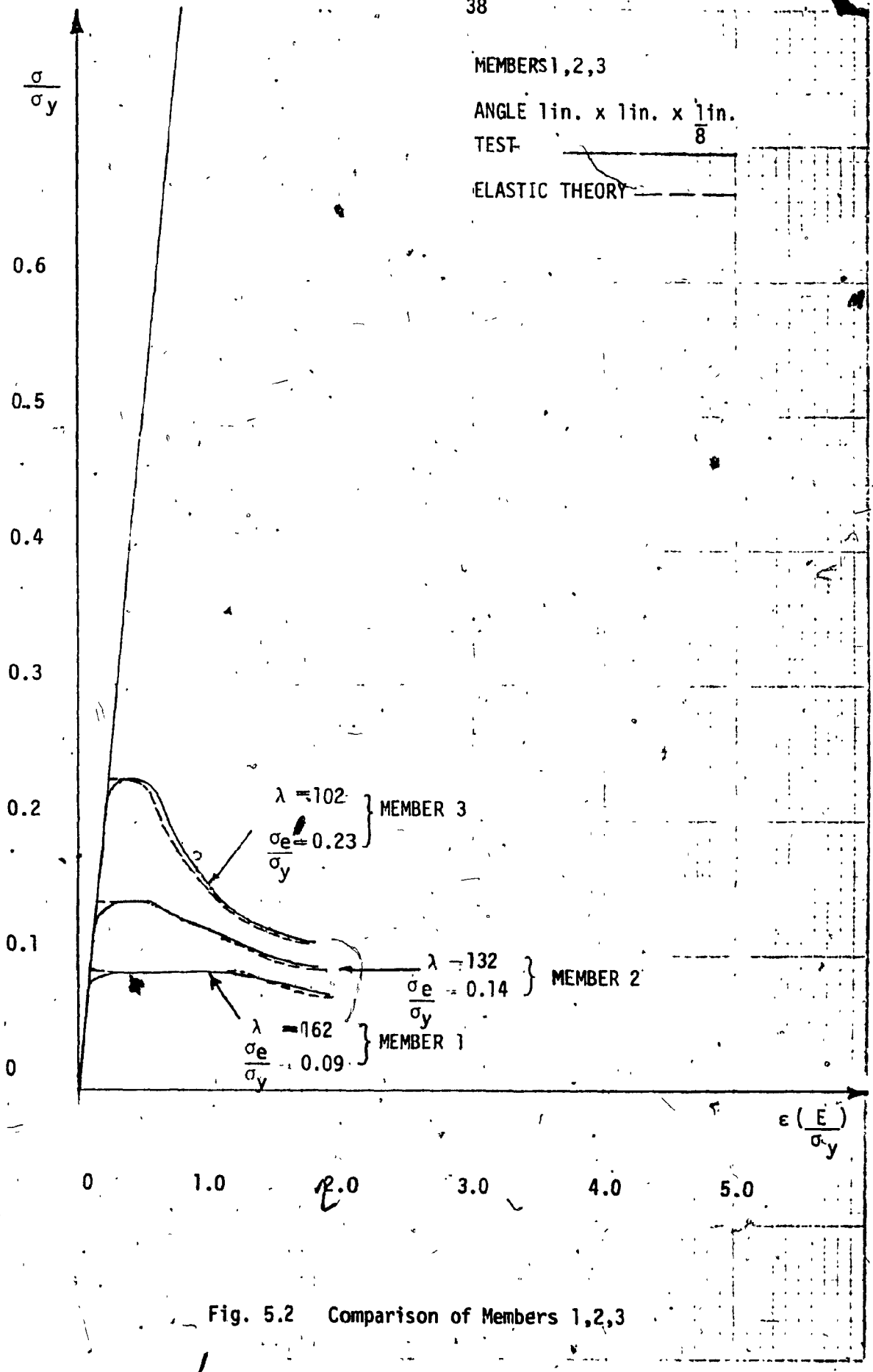

Fig. 5.2 Comparison of Members 1,2,3

5.1 DISCUSSION OF TEST RESULTS MEMBERS 1,2,3

Test results confirmed the post-buckling behaviour of the members as predicted by the Elastic Theory. The critical stress was calculated from the test values, by the Southwell method for member 2. This value was the same as the Euler stress, Fig. 5.2.

Tests showed that the post-buckling plateau increases with the slenderness ratio. Drop in load, after attaining a maximum, with axial deformation was sharper for less slender strut (member 3) than for members 1 and 2. All members buckled before reaching the Euler load. Test values of δ below the Euler load were different from the values as obtained from $\delta = \frac{PL}{AE}$.

Test curves were plotted by using $\delta = \frac{PL}{AE}$ below the Euler load. The difference between this value and the test value was assumed to be due to secondary deformations, and the same difference for a given stress level was subtracted for values beyond the buckling stress.

TABLE 5.5

MEMBER 4, BEARING 2

TEST RESULTS

P kips	δ in.	MEMBER PROPERTIES	$\frac{\sigma}{\sigma_y}$
		CIRCULAR BAR	
0.15		DIA = ½ in.	
0.3		A = 0.197 sqin.	
0.4		L = 22 in.	
0.5		σ_y = 35 ksi	
0.6		E = 10^4 ksi	
0.7		I = 0.003 in^4	
0.75	0.0087	r = $\frac{D}{4}$ = .125in	0.108 *
0.7	0.0095		0.101
0.65	0.01	$\frac{L}{r}$ = 176	0.094
0.62	0.04		0.09
0.6	0.1375	$P_e = \frac{\pi^2 EI}{L^2}$	0.087
0.55	0.19		0.079
		$= \frac{296}{L^2}$	0.06
			0.05
		= 0.62 kips	
		$\sigma_e = \frac{0.62}{0.197}$	
		= 3.14 ksi	
		C = $\frac{D}{2}$	
		= 0.25	
		S = .78R^3	
		= 0.012 in^3	
		Z = 1.7x0.012	
		= 0.02 in^3	

TABLE 5.5 cont'd

MEMBER 4, BEARING 2

TEST RESULTS $\varepsilon\left[\frac{E}{\sigma_Y}\right]$ $=\delta \times 13.0$	ELASTIC THEORY $\varepsilon\left[\frac{E}{\sigma_Y}\right]=\frac{\sigma}{\sigma_Y}+\frac{\sigma_R}{4\sigma_Y}\left[\frac{\sigma_Y}{\sigma}-1\right]^2\frac{r^2}{c^2}$ $=\frac{\sigma}{\sigma_Y}+.022\left[\frac{\sigma_Y}{\sigma}-1\right]^2 .25$	PLASTIC THEORY $\varepsilon\left[\frac{E}{\sigma_Y}\right]=\frac{\sigma}{\sigma_Y}+\frac{\sigma_R}{4\sigma_Y}\left[\frac{\sigma_Y}{\sigma}-\frac{\sigma}{\sigma_Y}\right]^2\frac{I^2}{I^2}\times r^2$ $=\frac{\sigma}{\sigma_Y}+.022\left[\frac{\sigma_Y}{\sigma}-\frac{\sigma}{\sigma_Y}\right]^2 .69$
* 0.114		
0.124		
0.13		
0.52	0.65	1.93
1.78	0.69	2.06
2.47	0.826	2.4

TABLE 5.6

MEMBER 5, BEARING 2

TEST RESULTS

P kips	δ in.	MEMBER PROPERTIES	$\frac{\sigma}{\sigma_y}$
0.15		CIRCULAR BAR	
0.30		DIA = ½ in.	
0.4		A = 0.197 sqin.	
0.6		L = 16 in.	
0.75		σ_y = 35 ksi	
1.0		E = 10^4 ksi	
1.15		I = 0.003 in^4	
1.3		r = 0.125 in	
1.5		$\frac{L}{r}$ = 64	
1.55			
1.60	0.021	$Pe = \frac{\pi^2 EI}{L^2}$	0.232
1.5	0.021	$= \frac{296}{L^2}$	0.217
1.3	0.025		0.188
* 1.2	0.0551	= 1.15 kips	0.174
1.1	0.0853	$\sigma e = \frac{1.15}{0.197}$	0.159
1.0	0.1225		0.145
0.85	0.165	= 5.86 ksi	0.123
0.75	0.1975	$C = \frac{D}{2}$	0.108
		= 0.25 in	
		S = 0.012 in^3	
		Z = 1.7x.012	
		= 0.02 in^3	

TABLE 5.6 cont'd

MEMBER 5, BEARING 2

TEST RESULTS $\varepsilon\left[\frac{E}{\sigma_Y}\right]$ $=6\times17.8$	ELASTIC THEORY $\varepsilon\left[\frac{E}{\sigma_Y}\right]=\frac{\sigma}{\sigma_Y}+\frac{\sigma_B}{4\sigma_Y}\left[\frac{\sigma_Y}{\sigma}-1\right]^2\frac{r^2}{c^2}$ $=\frac{\sigma}{\sigma_Y}+.042\left[\frac{\sigma_Y}{\sigma}-1\right]^2.25$	PLASTIC THEORY $\varepsilon\left[\frac{E}{\sigma_Y}\right]=\frac{\sigma}{\sigma_Y}+\frac{\sigma_B}{4\sigma_Y}\left[\frac{\sigma_Y}{\sigma}-\frac{\sigma}{\sigma_Y}\right]^2\frac{Z^2}{I^2}\times r^2$ $=\frac{\sigma}{\sigma_Y}+.042\left[\frac{\sigma_Y}{\sigma}-\frac{\sigma}{\sigma_Y}\right]^2.69$
0.374		
0.374		
0.445		
* 1.02	0.24	1.07
1.55	0.45	1.24
2.13	0.51	1.46
2.84	0.65	2.00
3.52	0.81	2.53
	0.95	2.94
	1.92	
	2.63	

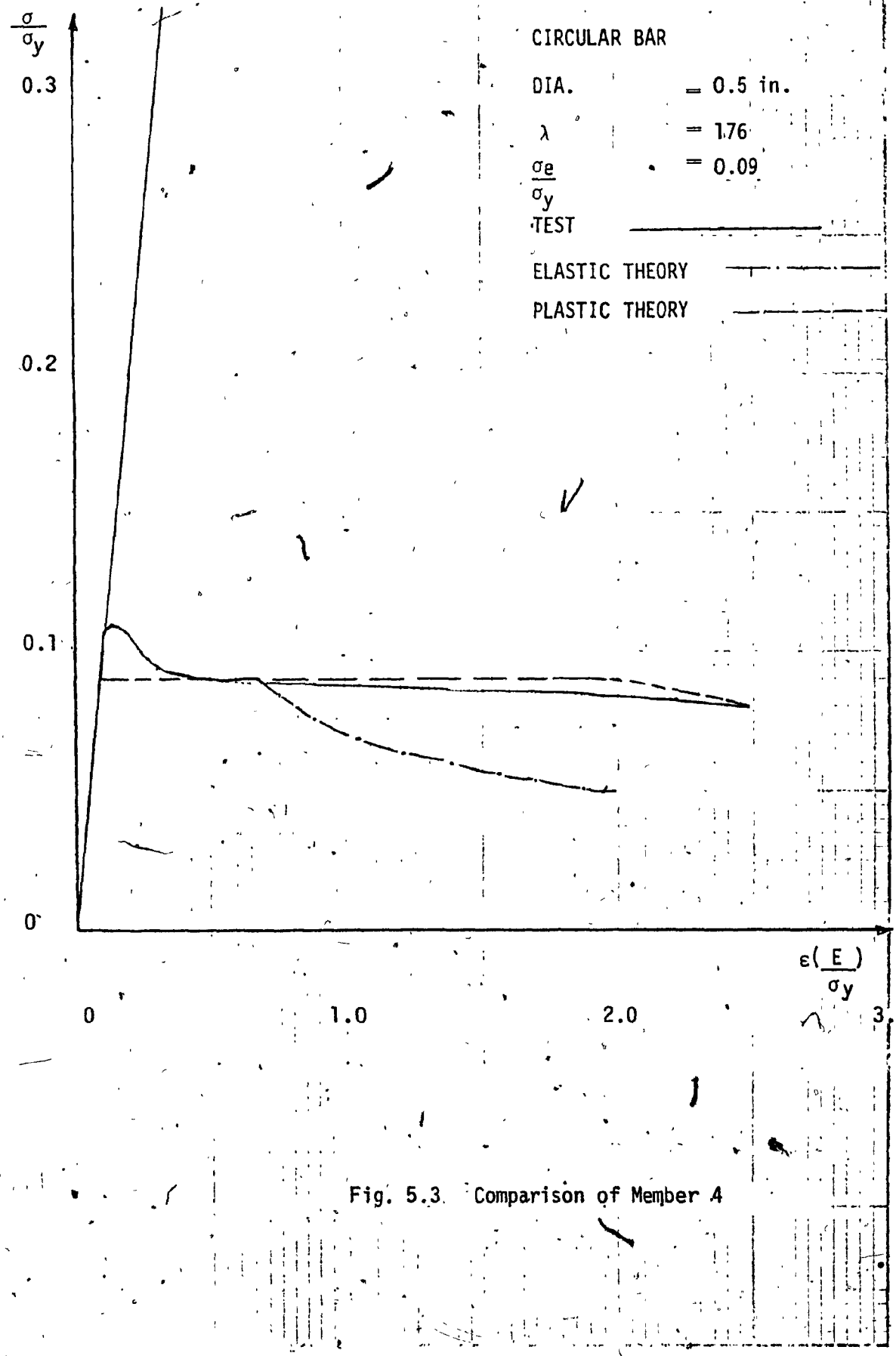

Fig. 5.3 Comparison of Member 4

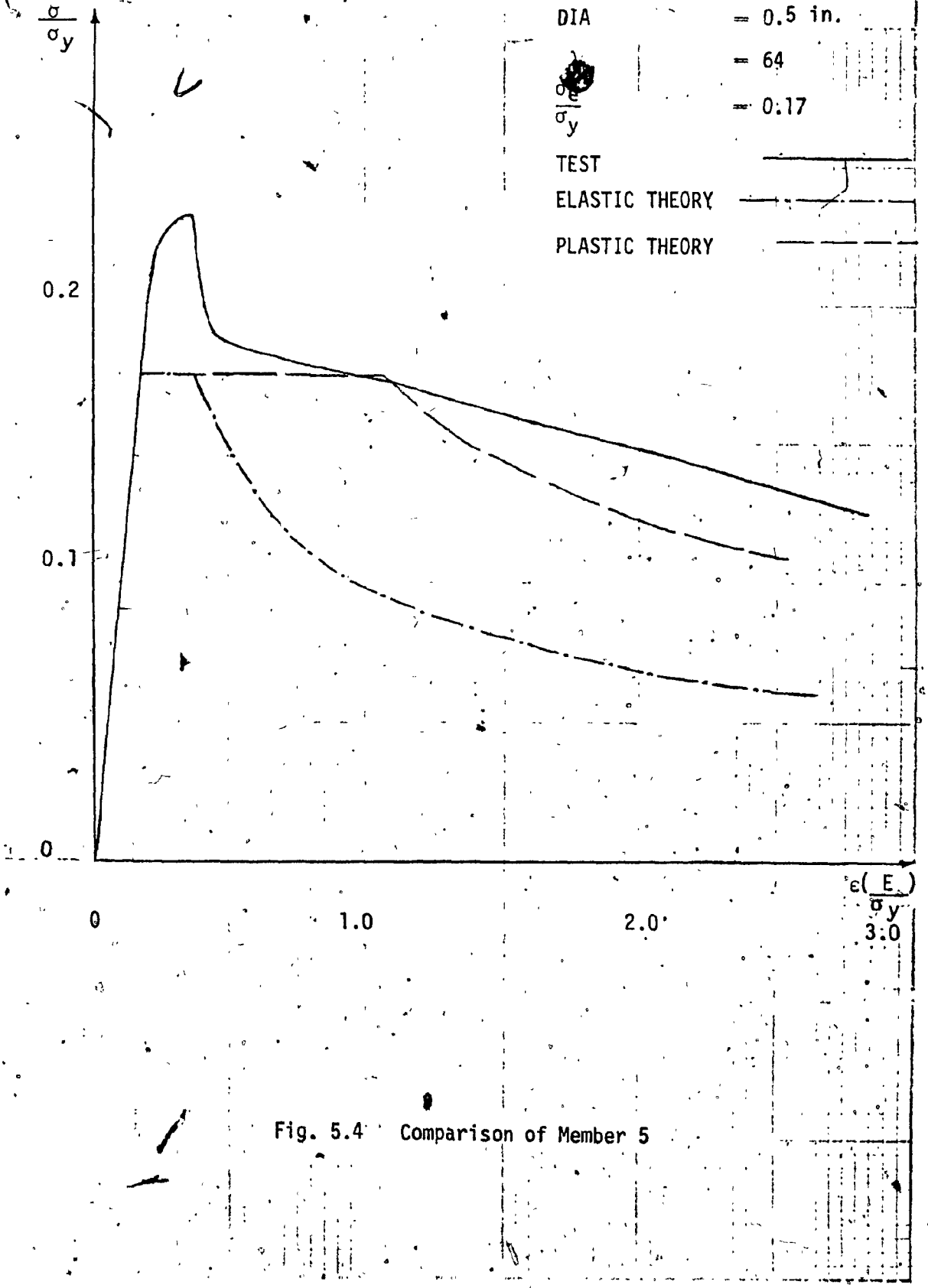

Fig. 5.4 Comparison of Member 5

5.2 DISCUSSION OF TEST RESULTS MEMBERS 4,5

The applied load attained for both the members was higher than the Euler load for a pin ended strut. The ball bearings, forced into the recessess in the ends of the member and in the bearing plates by the applied load, did not rotate freely and behaved as partially fixed. As the strut yielded, the ball bearings rotated and the load dropped to the Euler load. These were the only members to have reached fully plastic state. Test results were compared with the Elastic Theory and the Plastic Theory. The Plastic Theory compared favourably with the test results. The deviation between the test and theory, to a certain extent can also be due to the discontinuous rotations of end bearings.

The test curves were plotted by using $\delta = \frac{PL}{AE}$ values below Euler load and the rest of the values i.e. in the post-buckling state were adjusted to suit these corrected values.

TABLE 5.7

MEMBER 6, BEARING 3

TEST RESULTS

P kips	δ in.	MEMBER PROPERTIES	$\frac{\sigma}{\sigma_y}$
		SQUARE BAR	
0.3	.0024	0.5 x 0.5 in.	
0.5	.004	A = .25sq.in	
0.7	0.0056	L = 20 in	0.08
1.0	0.008	σ_y = 35 ksi	0.114
1.2	0.0096	E = 10^4 ksi	0.137
1.25	0.0225	I=0.0052in^4	0.142
1.15	0.047	r=0.145 in.	0.131 *
1.0	0.06	$\frac{L}{r}$=137.9	0.114
0.9	0.082	$Pe=\frac{\pi^2 EI}{L^2}$	0.103
0.8	0.105		0.091
0.7	0.155		0.08
		$=\frac{513.2}{20^2}$	
		= 1.28 kips	
		$\sigma e=\frac{1).28}{0.25}$	
		= 5.13 ksi	
		C = $\frac{.5}{2}$	
		= 0.25	
		S = 0.042 in^3	
		Z = 1.5x.042	
		= 0.0625in^3	

TABLE 5.7 cont'd

MEMBER 6, BEARING-3

TEST RESULTS $\varepsilon \left[\frac{E}{\sigma y}\right] = \delta \times 14.28$	ELASTIC THEORY $\varepsilon \left[\frac{E}{\sigma y}\right] = \frac{\sigma}{\sigma y} + \frac{\sigma_e}{4\sigma y}\left[\frac{\sigma y}{\sigma} - 1\right]^2 \frac{r^2}{c^2} = \frac{\sigma}{\sigma_y} + .036\left[\frac{\sigma y}{\sigma} - 1\right]^2 \times 0.33$
0.0343	
0.057	
0.079	
0.114	
0.137	
0.321	
* 0.67	0.65
0.85	0.83
1.14	1.0
1.49	1.26
2.21	1.65
	2.16

TABLE 5.8

MEMBER 7, BEARING 3

TEST RESULTS

P kips	δ in.	MEMBER PROPERTIES	$\frac{\sigma}{\sigma y}$
		SQUARE BAR	
0.3	0.0018	0.5 x 0.5in.	
0.5	0.003	A = 0.25sqin.	
0.7	0.0042	L = 15 in.	
1.0	0.006	σy = 35 ksi	0.114
1.5	0.009	$E = 10^4$ ksi	0.171
1.7	0.012	$I = 0.0052\ in^4$	0.194
2.0	0.018	r = 0.145 in.	0.228
2.2	0.0225	$\frac{L}{r} = 103.4$	0.251
2.0	0.026	$Pe = \frac{\pi^2 EI}{L^2}$	0.228 *
1.55	0.034		0.177
1.4	0.042		0.16
1.2	0.053	$= \frac{513.2}{L^2}$	0.137
1.1	0.063		0.125
1.0	0.075	= 2.28 kips	0.114
0.09	0.1	$\sigma_e = \frac{2.28}{25}$	0.102
0.8	0.1175	= 9.12 ksi	0.09
0.7	0.16	$S = 0.042in^3$	
		$Z = 1.5 \times .042$	
		$= 0.0625in^3$	

TABLE 5.8 cont'd

MEMBER 7, BEARING 3

TEST RESULTS $\varepsilon\left[\frac{E}{\sigma_y}\right] = \delta \times 19$	ELASTIC THEORY $\varepsilon\left[\frac{E}{\sigma_y}\right] = \frac{\sigma}{\sigma_y} + \frac{\sigma_e}{4\sigma_y}\left[\frac{\sigma_y}{\sigma} - 1\right]^2 \frac{r_2^2}{c^2}$ $= \frac{\sigma}{\sigma_y} + .065\left[\frac{\sigma_y}{\sigma} - 1\right]^2 \times .33$
0.0342	
0.057	
0.0798	
0.114	
0.171	
0.228	
0.342	
0.427	
0.496	0.47
0.646	0.63
0.798	0.75
1.0	0.98
1.19	1.16
1.42	1.40
1.9	1.63
2.2	2.2
3.04	

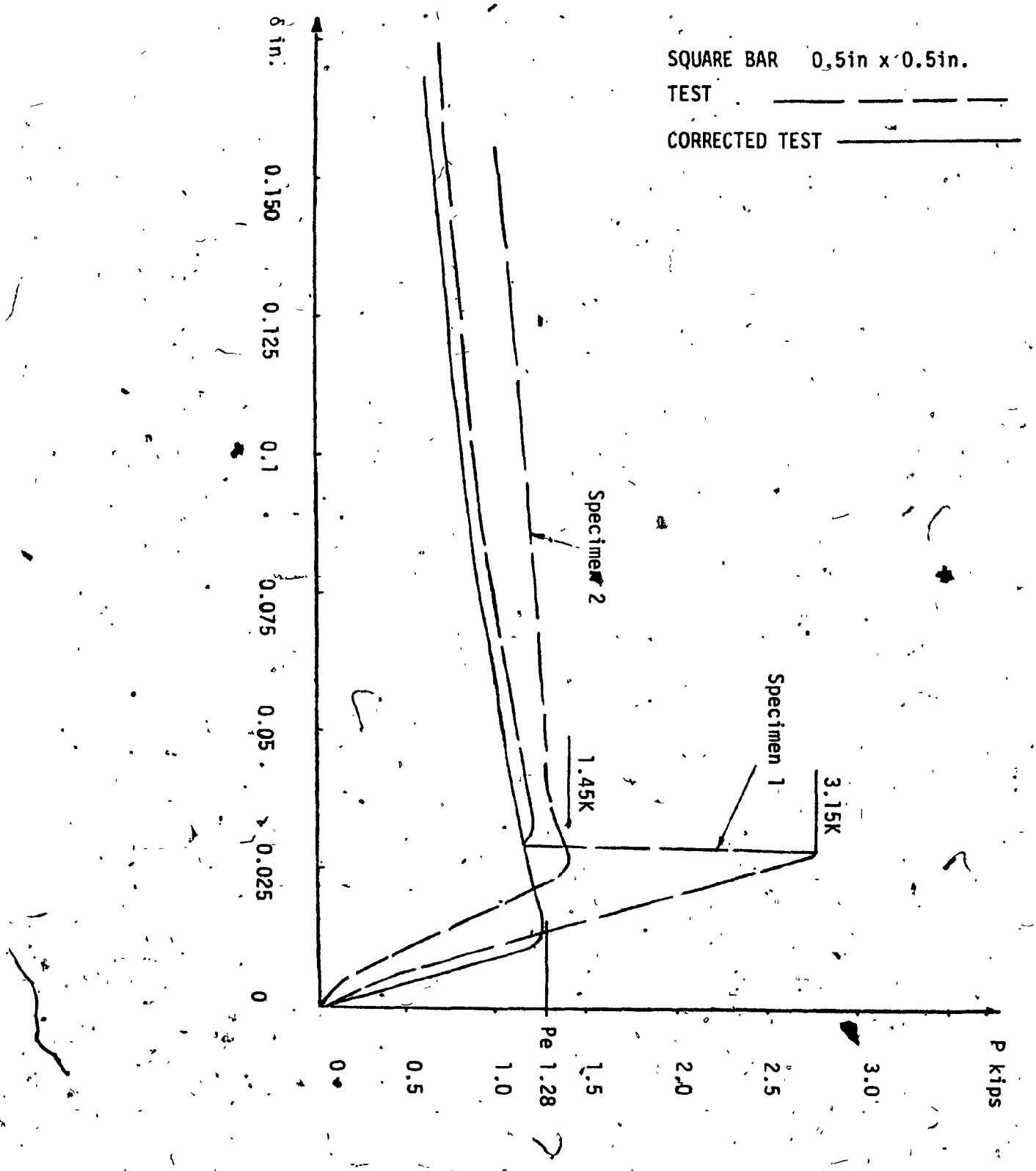

Fig. 5.5 Test Curve and Corrected Test Curve for member 6.

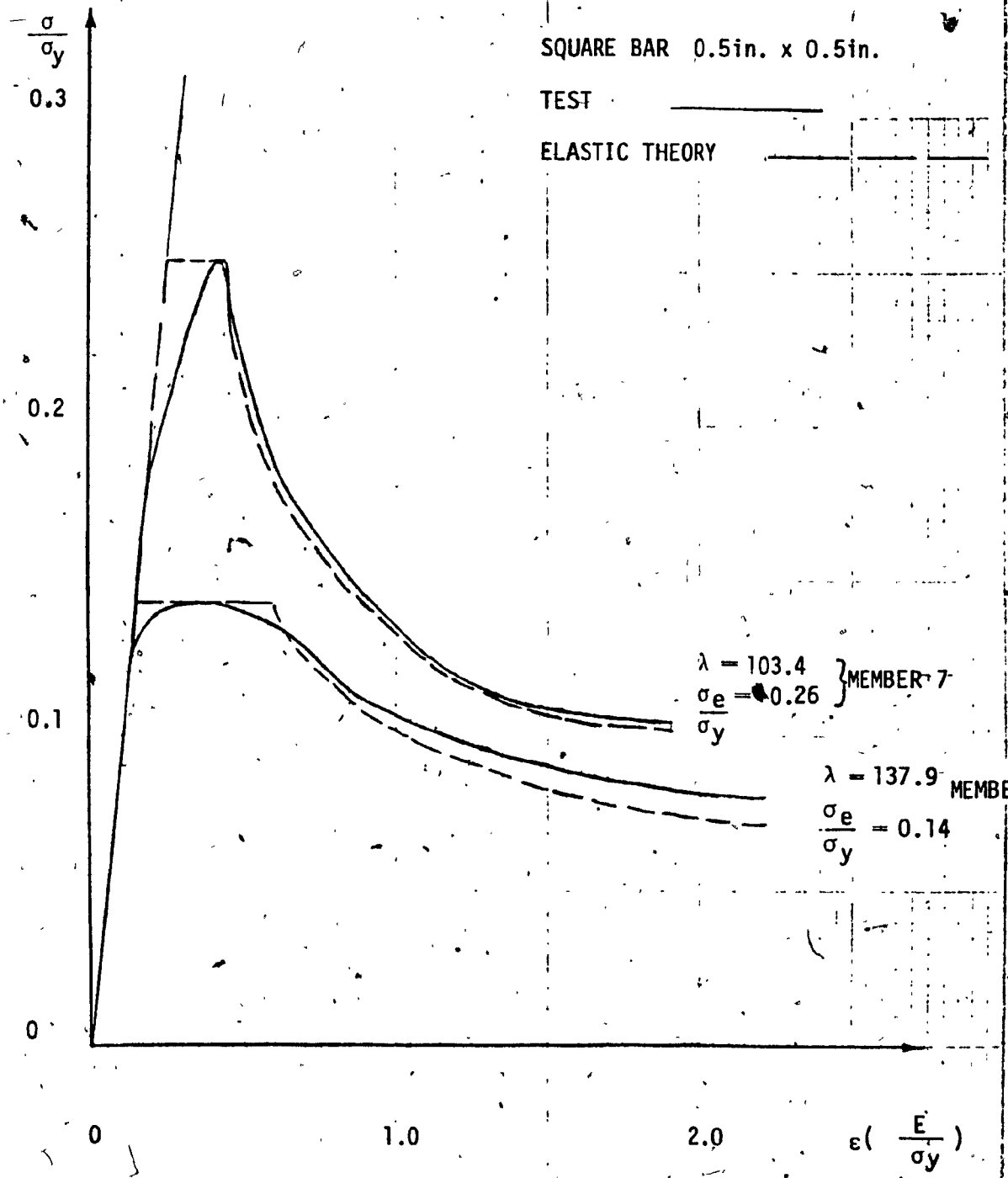

Fig. 5.6 Comparison Members 6,7

5.3 DISCUSSION OF TEST RESULTS

MEMBERS 6,7

Two specimens were tested for each case. Despite the precautions taken the members behaved as partially fixed before buckling, but each time after buckling the load dropped closer to the Euler value for pinned ends. The post-buckling behaviour was similar each time.

Test values of δ were different from those obtained by using $\delta = \frac{PL}{AE}$ below the Euler load. This difference in values at any given stress level was adjusted for values beyond the buckling stress and a corrected test curve was plotted Fig. 5.6. This procedure was adopted for both members. The values as obtained from this curve were found to be in close agreement with the Elastic Theory.

5.4 DISCUSSION OF TEST RESULTS

GENERAL

All the members tested gave values different from the Hooke's law in the elastic state. The difference in values in some cases was more than double. The strain of the machine was tested and found to be too small to be of any significance and was therefore ignored. Test values extracted from Schmidt (1) also deviated from the Hooke's law. No reasonable and satisfactory explanation could be given for the difference in values obtained. This difference was assumed to be due to secondary deformations. Test results were plotted assuming that the member obeyed Hooke's law in the elastic state. All experiments were conducted with utmost care. Although the machines were fully mechanised, the members had to be located straight and centrally by eye. The deviation of the behaviour of the bearings from a true pin end bearing and the uncertainty of the location of the vertical axis of the member in relation to the loading axis contributed to the disparity between test and 'theory.'

TABLE, 5.9

COMPARISON WITH SCHMIDT (1) TEST

TEST RESULTS FROM SCHMIDT (1)

P kips	$\frac{\sigma}{\sigma y}$	MEMBER PROPERTIES
		CIRCULAR HOLLOW TUBE
0.3		A = 0.086 sq.in.
0.7		L = 11. 89
1.1		σy = 40 ksi
1.55		E = 7.22 ksi
2.0	0.58	σ_e = 34 ksi
1.80	0.52	
1.63	0.47	
1.5	0.44	
1.24	0.36	
1.12	0.33	
1.0	0.29	
0.9	0.26	
0.8	0.25	

TABLE 5.9 cont'd

TEST RESULTS FROM SCHMIDT (1)	ELASTIC THEORY
δ in.	$\varepsilon\left[\frac{E}{\sigma_y}\right] = \frac{\sigma}{\sigma_y} + \frac{\sigma_e}{4\sigma_y}\left[\frac{\sigma_y}{\sigma} - 1\right]^2 \frac{r^2}{c^2}$ $\delta = .07\left[\frac{\sigma}{\sigma_y} + .22\left(\frac{\sigma_y}{\sigma} - 1\right)^2 .5\right]$
0.05	.044
0.06	.043
0.07	.043
0.08	.043
0.1	.049
0.12	.057
0.14	.066
0.16	.08
0.2	.087

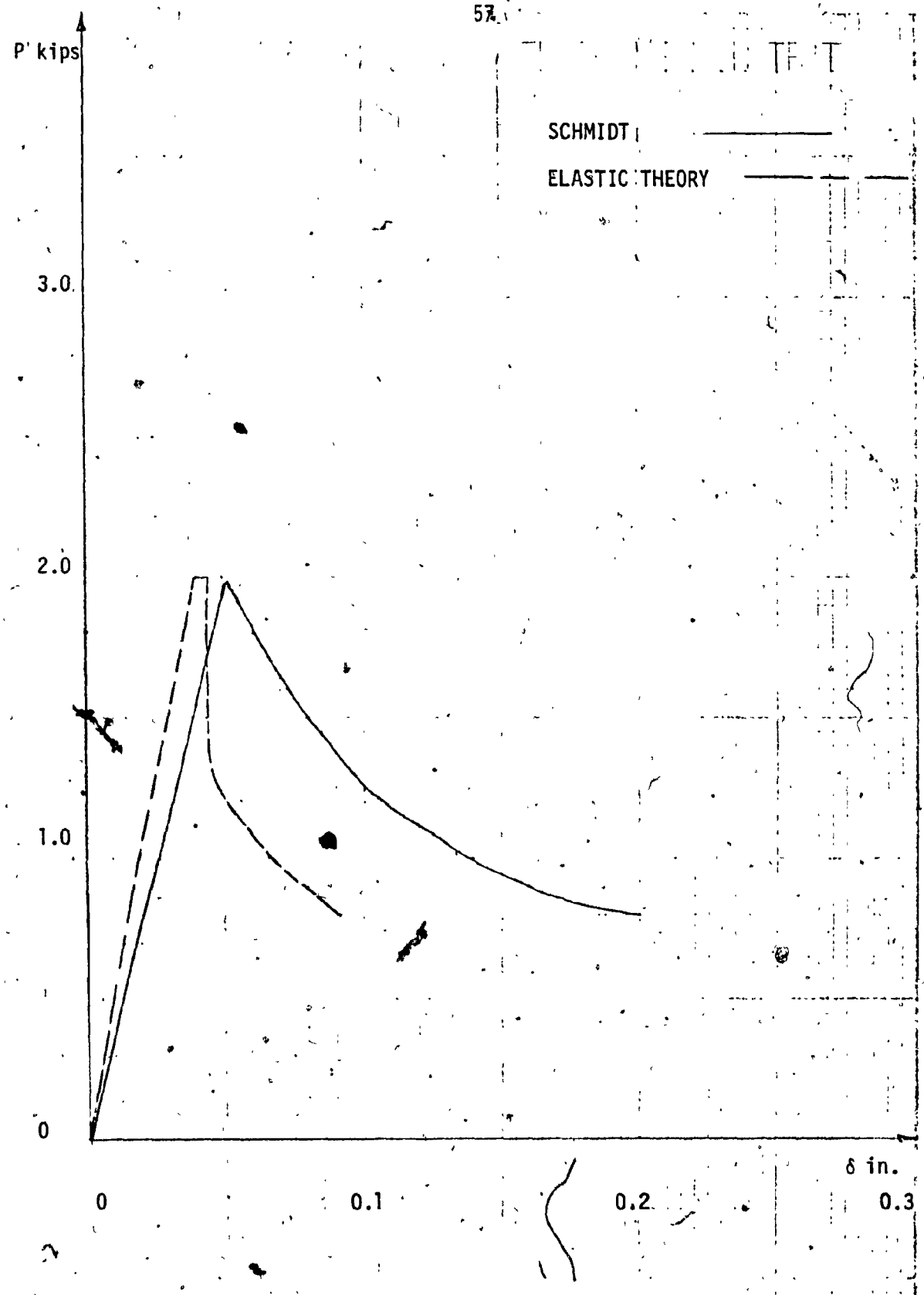

Fig. 5.7 Comparison with Schmidt (1) Test

5.5 COMPARISON WITH EARLIER WORKS

The δ values in the post-buckling state, as obtained from Schmidt (1) curve Fig. 2.1, are different from the 'Theory'. This may be partially due to the difference in values of δ as extracted from the curve below the Euler load and the values as obtained from $\delta = \frac{PL}{AE}$ These values of δ were not corrected but were plotted in Fig. 5.7 as extracted from Fig. 2.1. The two curves exhibit similar post-buckling behaviour.

Elastic Theory curves plotted in Fig. 3.4 show qualitative behaviour similar to the curves by Wolf (2) as shown in Fig. 3.4.

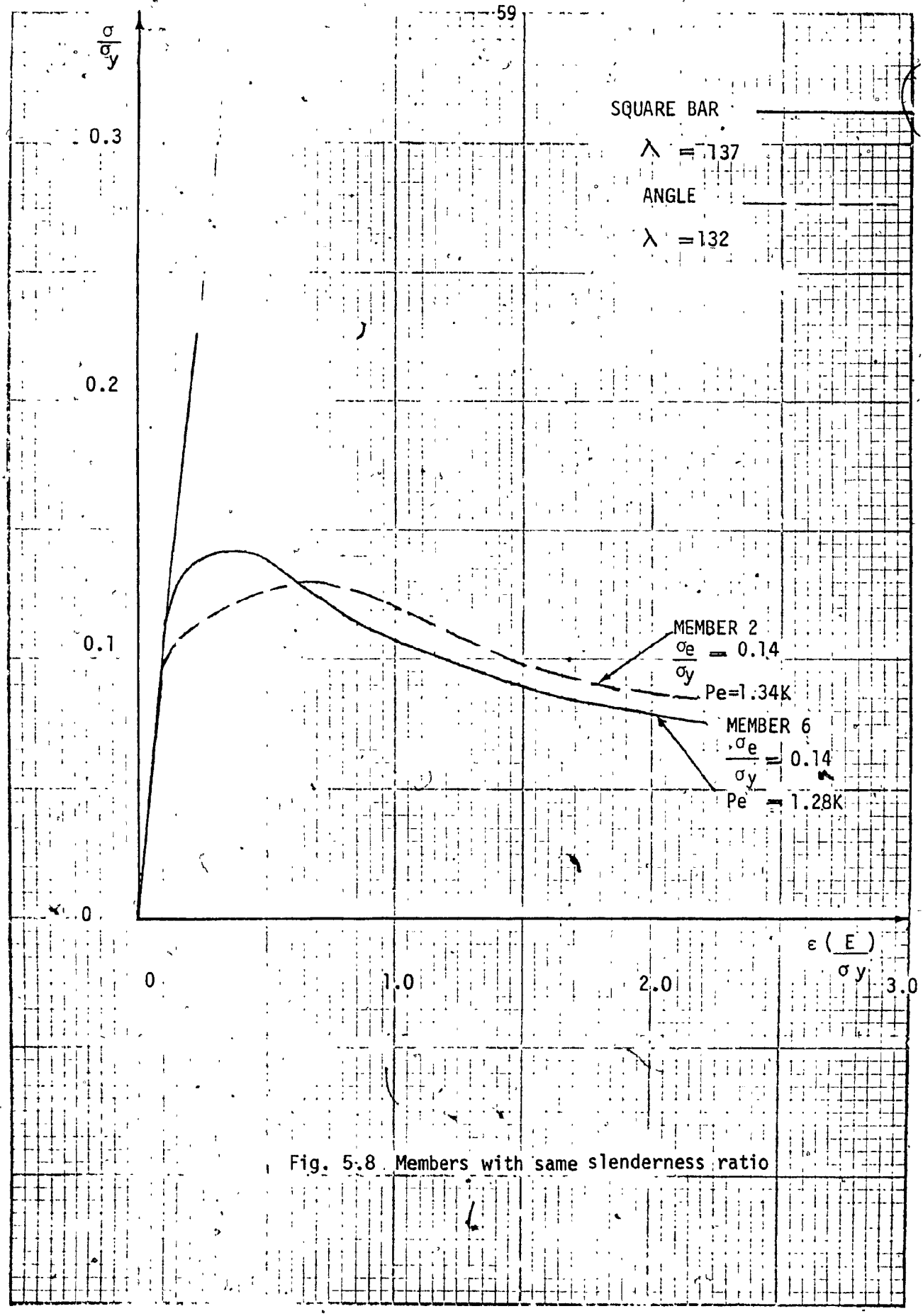

Fig. 5.8 Members with same slenderness ratio

CHAPTER 6

CONCLUSIONS

CHAPTER 6

CONCLUSIONS

A simple procedure for studying the load-shortening relationship of a pin ended axially loaded strut throughout its loading history has been suggested.

Tests were conducted to study experimentally the behaviour of the struts and the results were compared with the 'theory'.

The method was also compared with the existing work on the post-buckling behaviour of struts.

Test results obtained lie between the Plastic Theory as the upper bound and Elastic Theory as the lower bound. In the cross-sections tested, the behaviour of the most compact shape (circular bar) was closer to the Plastic Theory than to the Elastic Theory. Test values for member 5 were above the predicted Plastic theory values. This was probably because of the partially fixed end conditions obtained in this test. It is more likely that the Plastic Theory will predict the post-buckling behaviour of a compact shape better than the Elastic Theory, but this cannot be stated definitely. For design purposes the more conservative value may be chosen.

In the ultimate design of space-trusses the post-buckling

behaviour of the struts must be considered. The space truss may be designed so that the more slender members fail first because of the longer post-buckling plateau, and the last to fail should be the strongest members which can then contribute their full capacity.

The load/shortening relationship as predicted by Elastic Theory showed qualitative behaviour, similar to the results extracted from tests by Schmidt (1) Fig. 5.6.

Members with approximately same λ but different cross-sections exhibit similar qualitative post-buckling behaviour, Fig. 5.8.

The Elastic Theory curves Fig. 3.4 drawn, show similar behaviour to the curves drawn by Wolf (2).

The value of good experiments must be emphasised, as a small deviation from assumed conditions may introduce errors and more accurate tests should be conducted to study the behaviour of struts.

It follows that load/shortening relationship of an axially loaded pin ended strut may qualitatively be represented by the procedure presented in this study.

BIBLIOGRAPHY

BIBLIOGRAPHY

(1) Schmidt Lewis, C., Morgan Peter, R., Clarkson John A, Space Trusses with Brittle-Type Strut Buckling, Journal of the Structural Division, ASCE July 1976, pp. 1479-1492.

(2) Wolf John, P., Post-Buckled Strength of Large Space-Truss, Journal of the Structural Division ASCE July 1973, pp. 1709-1712.

(3) Schmidt, L.C., Alternative Design Methods for Parallel Chord Space Trusses, The Structural Engineer, Aug. 1972.

(4) Shanley, F.R., Elastic Column Theory', Journal of the Aeronautical Sciences, May 1947.

(5) Timoshenko and Gere, 'Theory of Elastic Statility'.

(6) Bleich, F., Buckling Strength of Metal Structures.

(7) Duberg John E., and Wilder Thomas W., III, Inelastic column behaviour, National Advisory Committee for Aeronautics, Technical note 2267.

(8) Clark, J.W., Plastic Buckling of Eccentrically loaded aluminum alloy columns, Proc. ASCE, Vol. 79, Oct. 1953, pp. 299-1, - 299 - 18.

(9) Ketter Robert L. and Kaminsky Edmund L., Plastic Deformation of Wide Flange Beam - Columns, Proc. ASCE, Vol. 79, Nov. 1953, pp. 330-1 - 330-53.

(10) Westergaard, H.M., and Osgood Wm. R., Strength of steel columns. ASME, May 1928.

(11) Norris and Wilbur, Structural Analysis.

(12) Shanley F.R., Strength of Materials.

(13) Gerard George, Introduction to Structural Stability Theory.

(14) Ketter L. Robert, Stability of beam columns above the elastic limit, Proc. ASCE, 81, Separate No. 692, May 1955.

(15) Ramberg Walter and Osgood William R., Description of stress-strain curves by three parameters, National Advisory Committee for Aeronautics, Technical note No. 902.

(16) Marsh Cedric and Sutherland J.G., Application of plastic theory to latticed aluminum frames, The Engineering Institute of Canada, Vol. 3, No. 3, Nov. 1959.

(17) Coates, Coutie, Kong, Structural Analysis.

(18) Lee George C. and Galambos Theodore V., Post-buckling strength of wide-flange beams, Proc. ASCE, Feb. 1962.